



Probing short-range correlations in asymmetric nuclei with quasi-free pair knockout reactions

Sam Stevens^a, Jan Ryckebusch^a, Wim Cosyn^{a,*}, Andreas Waets^b

^a Department of Physics and Astronomy, Ghent University, Belgium

^b Department of Physics and Astronomy, University of Leuven, Belgium



ARTICLE INFO

Article history:

Received 24 July 2017

Received in revised form 16 November 2017

Accepted 18 December 2017

Available online 22 December 2017

Editor: J.-P. Blaizot

Keywords:

Nuclear reaction theory

Nuclear short-range correlations

Asymmetric nuclei

ABSTRACT

Short-range correlations (SRC) in asymmetric nuclei with an unusual neutron-to-proton ratio can be studied with quasi-free two-nucleon knockout processes following the collision between accelerated ions and a proton target. We derive an approximate factorized cross section for those SRC-driven $p(A, p'N_1N_2)$ reactions. Our reaction model hinges on the factorization properties of SRC-driven $A(e, e'N_1N_2)$ reactions for which strong indications are found in theory-experiment comparisons. In order to put our model to the test we compare its predictions with results of $^{12}\text{C}(p, p'pn)$ measurements conducted at Brookhaven National Laboratory (BNL) and find a fair agreement. The model can also reproduce characteristic features of SRC-driven two-nucleon knockout reactions, like back-to-back emission of the correlated nucleons. We study the asymmetry dependence of nuclear SRC by providing predictions for the ratio of proton–proton to proton–neutron knockout cross sections for the carbon isotopes ^{9-15}C thereby covering neutron excess values $(N - Z)/Z$ between -0.5 and $+0.5$.

© 2017 The Authors. Published by Elsevier B.V. This is an open access article under the CC BY license (<http://creativecommons.org/licenses/by/4.0/>). Funded by SCOAP³.

1. Introduction

Many nuclear properties can be captured by the independent-particle model (IPM) that was developed in the fifties of the previous century and has not lost its attractiveness as a predictive and descriptive nuclear model ever since. The nucleus, however, turns out to be more than the linear sum of its nucleons and a rich range of nuclear features fall beyond the scope of the IPM. For example, nuclear long-range correlations (LRCs), here loosely defined as correlations that extend over distance scales of the order of the nuclear radius, give rise to exciting collective phenomena like giant resonances and halo nuclei. The corresponding excitation-energy scale of nuclear LRCs is well established and is of the order of MeVs. Nuclear short-range correlations (SRCs) [1–3] extend over distance scales of the order of the nucleon size, and are connected with substantially larger energy–momentum scales than the LRCs.

The scale separation between IPM, LRC and SRC effects is manifested in nuclear momentum distributions $n_A(k)$. The IPM can account for the strength below the Fermi momentum $k_F \approx 220 \text{ MeV}/c$. The impact of LRCs on the $n_A(k)$ at high nucleon mo-

menta is mainly confined to $k \gtrsim k_F$ [4] and the tensor component of the SRC is the major source of strength for the fat tails above the Fermi momentum [5]. This has important implications, for example, for the second moment $\langle k^2 \rangle$ of $n_A(k)$, that can be connected with the expectation value of the non-relativistic kinetic energy $\left\langle \frac{k^2}{2m_N} \right\rangle$. Indeed, in an IPM the majority component (most often neutrons) has a larger expectation value for the second moment $\langle k^2 \rangle$ than the minority component (most often protons). The dominant role of the tensor component in the SRC turns this picture upside down and provides the substantially larger values for the $\left\langle \frac{k^2}{2m_N} \right\rangle$ of the minority component (protons) [6–8]. This illustrates that there are important $(N - Z)$ asymmetry aspects to SRCs that are awaiting further explorations.

While being a fascinating phenomenon in itself, a full understanding of nuclear SRCs and its $(N - Z)$ asymmetry dependence is pivotal for studies of compact objects like neutron stars and of the nuclear equation of state [9,10]. The last couple of decades have marked significant growth in insight into the mass and isospin dependence of nuclear SRCs thanks to an experimental program of quasi-free two-nucleon knockout reactions with hadronic and electroweak probes [11–19]. Measuring the multi-fold cross sections for those reactions with at least four particles in the final state, is really challenging which made one to think about alternate ways

* Corresponding author.

E-mail addresses: Sam.Stevens@UGent.be (S. Stevens), Jan.Ryckebusch@UGent.be (J. Ryckebusch), Wim.Cosyn@UGent.be (W. Cosyn).

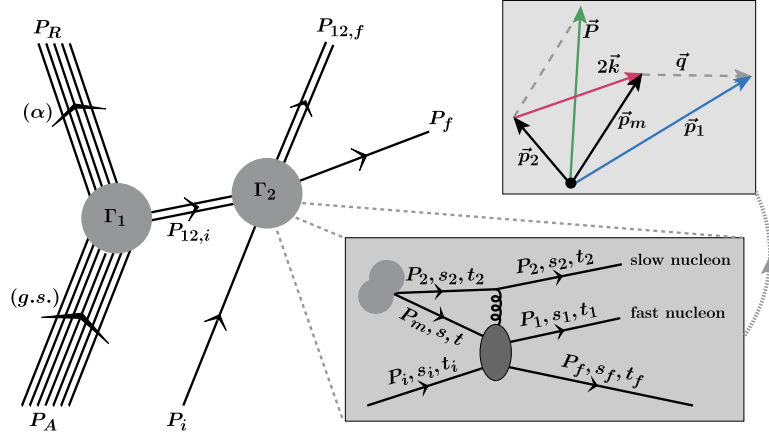


Fig. 1. Pictorial diagram of a kinematically complete $p(A, p'N_1N_2R^*)$ reaction in quasi-free kinematics. The reaction is induced by an accelerated ion A (four-momentum P_A) in its ground state colliding with a target proton (P_i). As a result, an SRC nucleon–nucleon (NN) pair gets ejected from the ion leaving a residual fragment R^* (P_R^*). The initial and final four-momenta of the SRC NN pair are $P_{12,i}$ and $P_{12,f}$. In the final state the pair consists of two asymptotically free nucleons with four-momenta $P_1(E_1, \vec{p}_1)$ and $P_2(E_2, \vec{p}_2)$. The recoiling target proton has four-momentum P_f . The residual nucleus R^* is created in a state designated by the quantum numbers α . The shaded boxes illustrate the momentum variables (top) and the spin-isospin (s, t) variables (bottom) used to describe the collision between an SRC NN pair and a proton in the IA.

of addressing SRC physics through nuclear reactions. Substantial progress in extracting the SRC physics from $A(e, e'N_1N_2)$ measurements has been recently made by investigating appropriate ratios of aggregated cross sections and observables against well-selected variables [5,19–21]. Thereby, proper kinematic cuts and selections have been key to success. Strong evidence for the proton–neutron dominance of SRC, for example, emerges from comparing measured $A(e, e'pp)/A(e, e'p)$ and $A(e, e'pn)/A(e, e'p)$ ratios [5]. The mass dependence of SRC could be addressed with the aid of measured $A(e, e'pp)/^{12}C(e, e'pp)$ and $A(e, e'pn)/^{12}C(e, e'pn)$ ratios [19]. The results of these studies provided strong evidence that for mid-heavy and heavy nuclei the aggregated impact of SRC roughly scales with the mass number ($\sim A$) and not with $\sim A^2$ as naively expected.

A remaining question, particularly important for understanding the physics of neutron stars for example, is how the SRC evolve with the asymmetry ($N - Z$) between the number of neutrons and protons. This question can be addressed with selected reactions at radioactive-beam facilities. Not only can one probe nuclei with an exotic ($N - Z$), the possibility to measure also the properties of the remnant nucleus, adds an additional layer of accuracy and detail that has not been achieved in most of the $A(e, e'N_1N_2)$ studies addressing SRC.

Due to new advanced techniques and equipment, the potential of quasi-free ($p, p'p$) single-nucleon knockout in inverse kinematics has been demonstrated to provide the means to study single-particle properties for short-lived nuclei [22–24]. Along the same lines, the development of a program for $(p, p'N_1N_2)$ SRC studies from short-lived nuclei with energies of the order of GeV per nucleon is discussed in the community. The success of studies using nucleon knockout reactions in quasi-free kinematics very much hinges on the availability of an approximate expression for the multi-fold cross sections. For example, the quasi-free hypothesis [25,26] has proven its great value and effectiveness in studies of the single-particle properties of nuclei with $(p, p'p)$ reactions. The quasi-free hypothesis requires that the transferred energy is large compared to the average binding energy and that the ejected nucleon N carries away most if not all of the transferred energy and momentum. The availability of a factorized approximate form for the cross sections, is particularly important in the planning phase of the experiments. For example, it is pivotal in order to get realistic estimates of the expected count rates. The main purpose of this paper is to provide a factorized expression for the SRC driven

quasi-free $p(A, p'N_1N_2R^*)$ reaction. We build our reaction model on a formalism that resulted in a factorized expression for exclusive $A(e, e'N_1N_2)R^*$ reactions that has been well tested in several theory-experiment comparisons [19–21,27–29]. Thereby we establish a connection between the correlation functions that account for nuclear SRC effects in the nuclear momentum distributions $n_A(k)$ and the two-nucleon knockout cross sections.

2. Formalism

We now develop an approximate but realistic framework to compute cross sections for $p(A, p'N_1N_2R^*)$ reactions (see Fig. 1 for momenta and spin-isospin labels). Our model applies to reactions where the accelerated ion's energy is sufficiently large to adopt the quasi-free hypothesis [25,26] that justifies both the impulse approximation (IA) and the spectator approximation (SA). The IA implies that the target proton interacts with a single nucleon in the SRC NN pair. In the SA only the correlated pair in the accelerated ion gets directly involved in the proton collision process and all other nucleons act as spectators [30]. The quasi-free reaction picture for $p(A, p'N_1N_2R^*)$ is schematically shown in Fig. 1. As is commonly the case with quasi-free processes, the transition matrix element \mathcal{M} can be approximately factored in a nuclear-structure (\mathcal{M}_1) and a nuclear-reaction (\mathcal{M}_2) part

$$\begin{aligned} \mathcal{M}(P_i + P_A \rightarrow P_f + P_{12,f} + P_R^*) \\ \approx \mathcal{M}_1(\Gamma_1; P_A \rightarrow P_R^* + P_{12,i}) \\ \times \mathcal{M}_2(\Gamma_2; P_{12,i} + P_i \rightarrow P_{12,f} + P_f). \end{aligned} \quad (1)$$

The vertex Γ_1 encodes at given kinematics the probability of removing a bound SRC NN pair from the accelerated ion. Reaction vertex Γ_2 describes proton scattering from an SRC NN pair resulting in three asymptotically free nucleons. For the calculation of the amplitude of the Γ_2 vertex (see inset of Fig. 1) we build on our derivations of a factorized cross section for electro- and photo-induced SRC NN pair knockout reactions [19–21,27,29]. Thereby, the transferred momentum $\vec{q} = \vec{p}_i - \vec{p}_f$ is fully absorbed by a single nucleon (the so-called “fast nucleon”) in the SRC NN pair. The other nucleon in the SRC NN pair is referred to as the “slow nucleon” and is ejected as a result of the “broken” correlation. In the projectile frame (PF), that is the rest frame of the accelerated

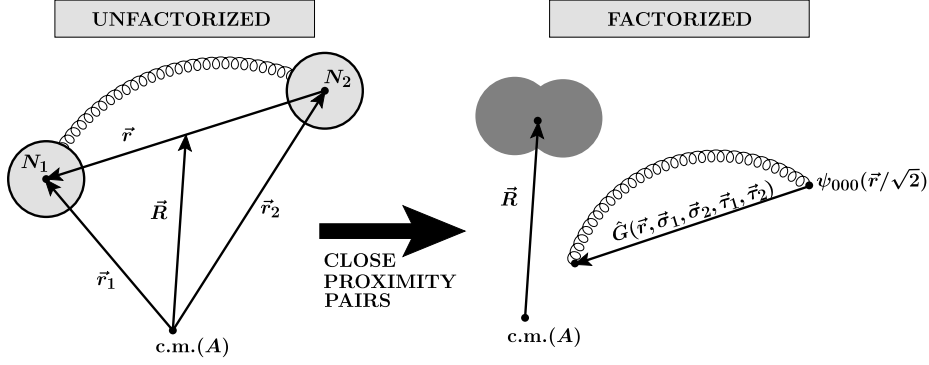


Fig. 2. Schematic representation of the spatial coordinates of a correlated NN pair. After projecting on close-proximity pairs, the dependence on the c.m. and relative coordinates can be factorized.

ion A , the missing energy E_m and missing momentum \vec{p}_m in the Γ_2 interaction are defined as

$$E_m = (E_1 + E_f - E_i - m_{N_1})_{\text{PF}}, \quad \vec{p}_m = (\vec{p}_1 + \vec{p}_f - \vec{p}_i)_{\text{PF}}, \quad (2)$$

where m_{N_1} is the mass of the fast nucleon. In the IA, \vec{p}_m corresponds with the momentum of the nucleon that scatters with the target proton. Ignoring medium modifications, the collision between the fast nucleon in the SRC NN pair and the proton target can be modeled as free nucleon–proton scattering

$$(P_m \equiv (E_m + m_{N_1}, \vec{p}_m), s, t) + (P_i, s_i, t_i) \rightarrow (P_1, s_1, t_1) + (P_f, s_f, t_f), \quad (3)$$

with s_j and t_j the spin and isospin projections of the nucleon j .

Given the possibility of detecting all final-state fragments in radioactive beam experiments, we compute the amplitude for given angular momentum and isospin of the ion ($= J_A T_A$) and of the residual fragment ($= J_R T_R$) under conditions that allow one to identify the slow nucleon and the isospins of all asymptotically free nucleons. The transition matrix element of Eq. (1) involves a summation over all allowed J, T combinations of the SRC NN pair and is evaluated in the PF

$$\begin{aligned} \mathcal{M} = & \frac{1}{\sqrt{2}} \sum_{JMTM_T} \sqrt{\mathcal{Z}(\Gamma_1)} \langle J_R M_R J M | J_A M_A \rangle \\ & \times \langle T_R M_{T,R} T M_T | T_A M_{T,A} \rangle \\ & \times \left\langle \frac{1}{2} t_1 \frac{1}{2} t_2 \middle| T M_T \right\rangle \sqrt{\frac{E_m m_{N_1}}{(E_m + m_{N_1}) m_{N_2}}} \sum_s M_{NN \rightarrow NN}^{pN_1} \frac{1}{(2\pi)^3} \\ & \times \int d\vec{R} d\vec{r} e^{-i\vec{p} \cdot \vec{R}} e^{-i\vec{k} \cdot \vec{r}} \langle \vec{R}, \vec{r}; s t_1, s_2 t_2 | (\beta\gamma) JMTM_T \rangle_{\text{SRC}}, \end{aligned} \quad (4)$$

with

$$\mathcal{Z}(\Gamma_1) \equiv \mathcal{Z}(\Gamma_1; J_R T_R, J T) = \frac{A(A-2)}{\mathcal{N}_{A,\text{corr}} \mathcal{N}_{R,\text{corr}}} \frac{\mathcal{S}(J_R T_R, J T, \beta\gamma)}{N_J N_T N_{J_R} N_{T_R}}. \quad (5)$$

Here, $\mathcal{S}(J_R T_R, J T, \beta\gamma)$ is a spectroscopic factor, N_J, N_T, N_{J_R} and N_{T_R} denote the number of possible quantum numbers for the SRC NN pair, and $\mathcal{N}_{A,\text{corr}}$ and $\mathcal{N}_{R,\text{corr}}$ are normalization factors. The first three factors in the above expression for the amplitude \mathcal{M} find their origin in the vertex Γ_1 . In the derivation of Eq. (4), the normalization of states is treated relativistically, whereas the dynamics is treated non-relativistically through wave functions evaluated in

the PF. The initial relative and c.m. momenta of the SRC NN pair (see also Fig. 1) are defined as

$$\vec{P} \equiv \vec{p}_{12,i}^{\text{cm}} = \vec{p}_m + \vec{p}_2, \quad \vec{k} \equiv \vec{p}_{12,i}^{\text{rel}} = \frac{\vec{p}_m - \vec{p}_2}{2}. \quad (6)$$

The corresponding conjugated c.m. and relative coordinates read

$$\vec{R} = \frac{\vec{r}_1 + \vec{r}_2}{2}, \quad \vec{r} = \vec{r}_1 - \vec{r}_2, \quad (7)$$

with \vec{r}_1 and \vec{r}_2 (see Fig. 2) the spatial coordinates of the SRC NN pair in the projectile frame.

In the expression of Eq. (4), $M_{NN \rightarrow NN}^{pN_1}$ is the matrix element for elastic nucleon–nucleon scattering and the $|(\beta\gamma) JMTM_T\rangle_{\text{SRC}}$ determines the quantum state of the SRC NN pair. It is constructed as in Ref. [29] that contains a derivation of a factorized cross section of SRC-driven $A(e, e' N_1 N_2) R^*$. The SRC pair's state is modeled as a correlation operator acting on a normalized and anti-symmetric (nas) state of two IPM nucleons characterized by the quantum numbers $\beta = (n_\beta, l_\beta, j_\beta, t_\beta)$ and $\gamma = (n_\gamma, l_\gamma, j_\gamma, t_\gamma)$ respectively. As a result, the residual fragment's state α can be specified by a two-hole state $|\beta^{-1} \gamma^{-1}\rangle$ in the ground state of the initial nucleus. With these assumptions, one can write for the state of the SRC NN pair

$$\begin{aligned} |(\beta\gamma) JMTM_T\rangle_{\text{SRC}} \\ = \widehat{G}(\vec{r}, \vec{\sigma}_1, \vec{\sigma}_2, \vec{\tau}_1, \vec{\tau}_2) |n_\beta n_\gamma l_\beta l_\gamma (j_\beta j_\gamma) JM(t_\beta t_\gamma) TM_T\rangle_{\text{nas}}. \end{aligned} \quad (8)$$

We use harmonic oscillator (HO) single-particle states as they offer the possibility to separate the pair's relative and c.m. motion with the aid of Moshinsky brackets $(\dots)_{\text{Mos}}$. It has been numerically shown [8,19–21,27,29] that in evaluating expressions of the type (8) the major source of SRC strength stems from correlation operators acting on IPM pairs with relative quantum numbers $(n=0, l=0)$. This can be intuitively understood by noting that the probability of finding close-proximity IPM pairs is dominated by pairs in a relative $(n=0, l=0)$ state (see also Fig. 2). In Ref. [8] it was shown that across the nuclear chart about 90% of the fat tail in the $n_A(k)$ finds its origin in correlation operators acting on IPM pairs in a relative $(n=0, l=0)$ state.

This leads to the following approximate expression for the wave function of the SRC NN pair in coordinate space:

$$\begin{aligned} \langle \vec{R}, \vec{r} | (\beta\gamma) JMTM_T \rangle_{\text{SRC}} \\ \approx 2 \sum_{NLM_L M_S} C_{00JM}^{\beta\gamma}(S, M_S, N, M_L) \psi_{NLM_L}(\sqrt{2}\vec{R}) \\ \times \psi_{000}\left(\frac{\vec{r}}{\sqrt{2}}\right) \widehat{G}(\vec{r}, \vec{\sigma}_1, \vec{\sigma}_2, \vec{\tau}_1, \vec{\tau}_2) |(1-T) M_S, T M_T\rangle, \end{aligned} \quad (9)$$

where $\psi_{nlm_l}(\frac{\vec{r}}{\sqrt{2}})$ ($\psi_{NLM_L}(\sqrt{2}\vec{R})$) are HO eigenstates for the pair's relative (c.m.) motion and the following factor has been introduced

$$\begin{aligned} C_{00JM}^{\beta\gamma}(S, M_S, N, M_L) &= \left\langle 00, N(\varepsilon - 2N), (\varepsilon - 2N) \left| n_{\beta} l_{\beta}, n_{\gamma} l_{\gamma}, (\varepsilon - 2N) \right\rangle_{\text{Mos}} \right. \\ &\times \sum_{s_b, s_c} \sum_{m_b, m_c} \sum_{m_{\beta}, m_{\gamma}} \langle j_{\beta} m_{\beta} j_{\gamma} m_{\gamma} | JM \rangle \langle l_{\beta} m_b \frac{1}{2} s_b | j_{\beta} m_{\beta} \rangle \\ &\times \langle l_{\gamma} m_c \frac{1}{2} s_c | j_{\gamma} m_{\gamma} \rangle \langle \frac{1}{2} s_b \frac{1}{2} s_c | (1-T) M_S \rangle \\ &\times \langle l_{\beta} m_b l_{\gamma} m_c | (\varepsilon - 2N) M_L \rangle, \end{aligned} \quad (10)$$

with $\varepsilon = 2n_{\beta} + l_{\beta} + 2n_{\gamma} + l_{\gamma}$ the HO energy of the NN pair.

With respect to the correlation operator \hat{G} , the central (c), tensor ($t\tau$), and spin-isospin ($\sigma\tau$) terms are responsible for the majority of the nuclear SRC [8,20,29,31–35]

$$\begin{aligned} \hat{G}(\vec{r}, \vec{\sigma}_1, \vec{\sigma}_2, \vec{\tau}_1, \vec{\tau}_2) &= 1 - f_c(r) + f_{t\tau}(r) \hat{S}_{12}(\vec{\tau}_1 \cdot \vec{\tau}_2) \\ &+ f_{\sigma\tau}(r) (\vec{\sigma}_1 \cdot \vec{\sigma}_2) (\vec{\tau}_1 \cdot \vec{\tau}_2), \end{aligned} \quad (11)$$

with \hat{S}_{12} the tensor operator. The functions f_c , $f_{t\tau}$ and $f_{\sigma\tau}$ are the central, tensor and spin-isospin correlation functions. They are responsible for the fat tails in the nuclear momentum distributions and determine the SRC interaction strength at any given spin-isospin combination of the NN pair. All results contained in this paper are obtained with a set of correlation functions that we have systematically used and tuned in SRC-driven reaction studies [13] [15] [19] [28]. The $f_{t\tau}(r)$ and $f_{\sigma\tau}(r)$ correlation functions are from a variational calculation [33], the central correlation function $f_c(r)$ from the G-matrix calculations in nuclear matter [36].

After averaging over initial and summing over final polarization states, the combination of Eqs. (4), (9) and (11), leads to the following factorized differential cross section in the laboratory frame

$$\begin{aligned} \frac{d\sigma^{pN_1N_2}}{d\Omega_f dE_1 d\Omega_1 dE_2 d\Omega_2} &= 2^{|M_T|} \mathcal{K} \frac{d\sigma^{pN_1}}{dt} \\ &\times \left\{ \frac{E_2}{E_m + m_{N_1}} \sum_{JMT} \frac{\mathcal{Z}(\Gamma_1; J_R T_R, JT)}{(2J+1)(2T+1)} F_{JM,T}^{\beta\gamma}(\vec{P}, \vec{k}) \right\}_{\text{PF}} \end{aligned} \quad (12)$$

with \mathcal{K} a kinematic factor evaluated in the laboratory frame

$$\begin{aligned} \mathcal{K} &= \frac{1}{(2\pi)^8} \frac{(P_f \cdot P_1)^2 - m_p^2 m_{N_1}^2}{\sqrt{(P_i \cdot P_A)^2 - m_p^2 m_A^2}} m_A m_{R^*} \frac{P_f P_1 P_2}{E_R} \\ &\times \left| 1 - \frac{E_f \vec{p}_R \cdot \vec{p}_f}{E_R p_f^2} \right|^{-1}, \end{aligned} \quad (13)$$

$\frac{d\sigma^{pN_1}}{dt}$ (with $t \equiv (P_i - P_f)^2$) the cross section for free proton-nucleon scattering, determined at the off-shell kinematic invariants of the subprocess of Eq. (3), and the factor between curly brackets is evaluated in the projectile frame. The function $F_{JM,T}^{\beta\gamma}(\vec{P}, \vec{k})$ accounts for the SRC effects and can be factored into parts depending on the c.m. (\vec{P}) and relative (\vec{k}) momentum of the SRC pair (see also Fig. 2)

$$\begin{aligned} F_{JM,T}^{\beta\gamma}(\vec{P}, \vec{k}) &= \sum_{\mu=T-1}^{1-T} \left| \mathcal{F}^{(0)}[f_c - 3f_{\sigma\tau}](k) \mathcal{P}_{JMT\mu}^{\beta\gamma}(\vec{P}) \right. \\ &\left. - \delta_{T,0} 12\sqrt{2\pi} \mathcal{F}^{(2)}[f_{t\tau}](k) \right|^2 \end{aligned}$$

$$\times \sum_{m_l=-2}^2 \langle 2m_l 1\mu | 1(m_l + \mu) \rangle \mathcal{P}_{JMT(m_l+\mu)}^{\beta\gamma}(\vec{P}) Y_{2,m_l}(\Omega_k) \Big|^2. \quad (14)$$

Obviously, the relative-momentum part receives contributions from all three terms in the correlation operator of Eq. (11). At given k the strength attributed to the correlation function f is given by

$$\begin{aligned} \mathcal{F}^{(l)}[f](k) &= \frac{4\pi}{\sqrt{2l+1}} \\ &\times \left[\sum_{m_l'=-l'}^{l'} \left| \int \frac{d\vec{r}}{(2\pi)^{3/2}} e^{-i\vec{k}\cdot\vec{r}} \psi_{000}\left(\frac{\vec{r}}{\sqrt{2}}\right) Y_{l'm_l'}(\Omega) f(r) \right|^2 \right]^{1/2}. \end{aligned} \quad (15)$$

At given c.m. momentum \vec{P} the contribution to the $F_{JMT}^{\beta\gamma}(\vec{P}, \vec{k})$ is determined by

$$\begin{aligned} \mathcal{P}_{JMT\mu}^{\beta\gamma}(\vec{P}) &= \sum_N C_{00JM}^{\beta\gamma} (1-T, \mu, N, M-\mu) \\ &\times \int \frac{d\vec{R}}{(2\pi)^{3/2}} e^{-i\vec{P}\cdot\vec{R}} \psi_{NLM_L=(\varepsilon-2N)}^{\beta\gamma}(\sqrt{2}\vec{R}). \end{aligned} \quad (16)$$

3. Results

All results presented here use the cross-section form of Eq. (12) based on plane-wave dynamics of the impinging and ejected nucleons ignoring initial- and final-state interactions (IFSI). The FSI analysis of SRC-driven $A(e, e'N_1N_2)$ in [21] indicate that FSI mainly cause a reduction of the cross sections, without significantly changing their shape. For the cross sections with carbon beams we deduce an IFSI reduction factor of the plane-wave based cross sections of the order 0.05–0.1. In what follows we present results for SRC driven 2N knockout from the ^{9-16}C isotopes. The HO single-particle states of those nuclei are obtained from an analysis of the momentum distributions extracted from the $p(^{9-16}\text{C}, p'p)$ measurements of Ref. [23]. The values for the free proton-proton cross section $\frac{d\sigma^{pp}}{dt}$ in Eq. (12) are obtained from the SAID code [37,38] for laboratory kinetic energies below 3 GeV and from the parametrization of Ref. [39] for higher energies.

Fig. 3 displays the $p(^{10}\text{C}, p'pn)$ cross section in specific in-plane kinematics. Clearly, the bulk of the cross sections comes from pn knockout in configurations approaching back-to-back of the initial SRC pair. This feature emerges in several SRC investigations [5,19,21,40].

In order to test the validity of the factorized cross section derived in Sec. 2, we compare computed $^{12}\text{C}(p, p'pn)$ cross sections with experimental results obtained with the EVA spectrometer at BNL [16,41]. The kinematics is detailed in Ref. [42]. In order to match the kinematic areas of the calculations and the data we have adopted the kinematics cuts outlined in Ref. [16] and we used the data-driven pp differential cross section parametrization of Ref. [39]. We consider knockout of SRC pn pairs from the s and p shells in carbon. All results of Fig. 4 use Eq. (12) with the ejected neutron as the “slow” nucleon.

Obviously the calculations reproduce the change in the angular correlations for the opening angle between the nucleons in the pair between $p_2 < k_F$ and $p_2 > k_F$. In Fig. 4, we also show the $^{12}\text{C}(p, p'pn)$ cross section as a function of the longitudinal light-cone momentum fractions α_m and α_2 carried by the nucleons in the ejected SRC NN pair. With the \hat{z} -axis parallel to the beam, the α_j are defined as [43]

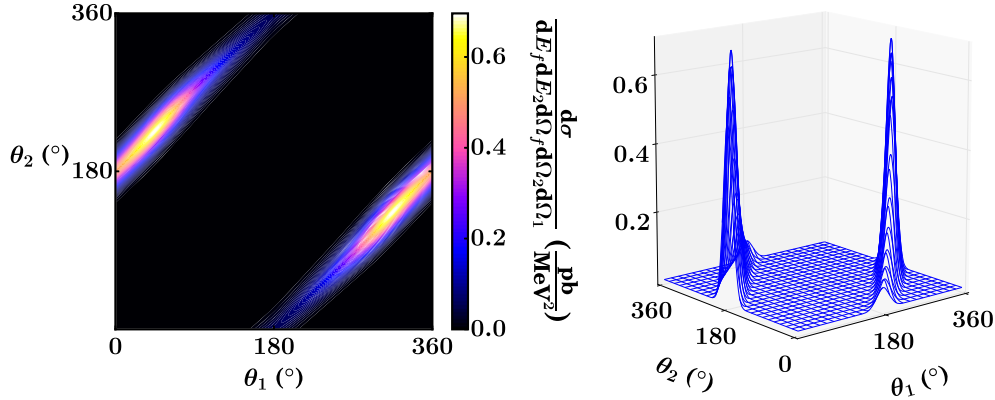


Fig. 3. The $p(^{10}\text{C}, p'pn)$ cross section for the knockout of an SRC pn pair as a function of the bound proton's (neutron's) PF angle θ_1 (θ_2) relative to the initial proton momentum \vec{p}_i . All particle momenta lie in the ion scattering plane, with laboratory momenta $p_A = 2.5$ A GeV and $p_f = 1.5$ GeV. The nucleons' initial momenta in the PF are $p_m = p_2 = 400$ MeV.

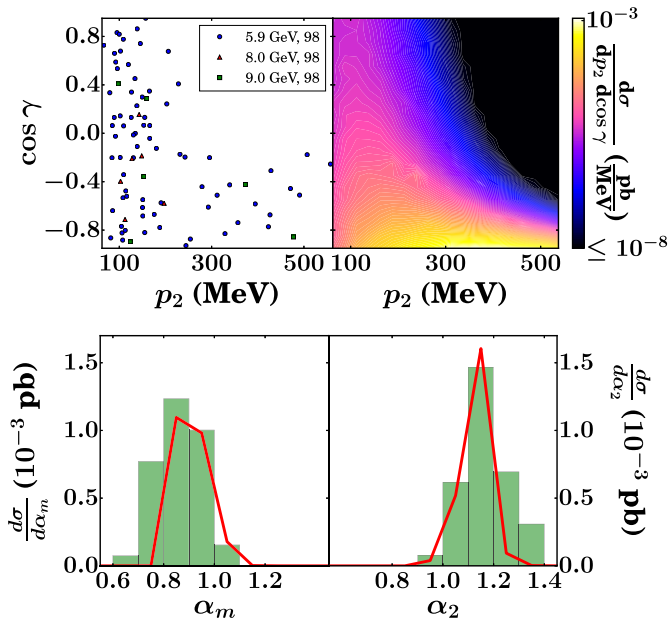


Fig. 4. Predictions for $^{12}\text{C}(p, p'pn)$ observables in the kinematics of Ref. [16]. Top: Heat map of pn knockout events as a function of the opening angle $\cos\gamma$ and the initial neutron momentum p_2 . We compare measured events (left panel adapted from Ref. [41]) with calculated cross sections (right panel). Bottom: The cross section as a function of the light-cone momentum fractions α_m and α_2 . We compare calculated cross sections (solid lines), to the histogram of the measured number of events [16]. As the data are provided as “counts” they are scaled in such a way that the mean of the two measured and computed cross-section peaks coincide.

$$\alpha_j = A \frac{E_j - p_{j,z}}{E_A - p_{A,z}}. \quad (17)$$

For high-energetic beams, the α_j are natural variables to characterize the nucleons' momentum distributions. In the PF ($P_A = (m_A, \vec{0})$) one finds [16]

$$\alpha_m \approx 1 + \frac{E_m - p_{m,z}}{m_{N_1}} \quad \text{and} \quad \alpha_2 \approx \frac{E_2 - p_{2,z}}{m_{N_2}}. \quad (18)$$

In Fig. 4 we compare the calculated cross sections with the measured number of events. As a supplementary consistency check, we apply the same scaling factor to the α_m and α_2 distributions. The shapes of both histograms are captured well by the calculated cross sections. The use of a unique normalization factor indicates that our model reproduces the relative cross sections $\frac{d\sigma}{d\alpha_m} / \frac{d\sigma}{d\alpha_2}$.

In order to derive the SRC pair probabilities from the cross section of Eq. (12), we define the function

$$P_{\beta\gamma}^{M_T}(\vec{P}, \vec{k}) = 2^{2|M_T|-1} \sum_{J M_T} \frac{1}{2J+1} \frac{1}{2T+1} F_{J M_T}^{\beta\gamma}(\vec{P}, \vec{k}), \quad (19)$$

that determines at given c.m. and relative momentum the cross section for removing a pair with given M_T . The ratio of pn to pp SRC pair probabilities at given k can be derived from the expressions (14), (15), (16) after integration over the c.m. momentum \vec{P} of the SRC pair. This operation results in

$$\begin{aligned} \mathcal{R}_{\frac{pn}{pp}}(k) &= \frac{\sum_{\beta\gamma} \int d\Omega_k d\vec{P} P_{\beta\gamma}^{M_T=0}(\vec{P}, \vec{k})}{\sum_{\beta\gamma} \int d\Omega_k d\vec{P} P_{\beta\gamma}^{M_T=1}(\vec{P}, \vec{k})} \\ &= \frac{1}{2} + \frac{3}{2} S_0 + 108 S_1 \left\{ \frac{\mathcal{F}^{(2)} f_{T\tau}(k)}{\mathcal{F}^{(0)} [f_c - 3f_{\sigma\tau}](k)} \right\}^2, \end{aligned} \quad (20)$$

where S_0 and S_1 depend on the quantum numbers of the impinging ion and are k -independent. The ratio of Eq. (20) can be connected to cross-section ratios accessible in $p(A, p'pN)$ experiments and is for example not sensitive to FSI effects in the SRC pair.

Fig. 5 shows predictions for the k -dependence of the ratio (20) and its inverse for different carbon isotopes. Three regions in the relative momentum can be discerned. For $k < k_F$ the pp to pn SRC pair fractions are constant and are determined by $\left(\mathcal{R}_{\frac{pn}{pp}}(k) = \frac{1}{2} + \frac{3}{2} S_0\right)$. The number of $n=0, l=0$ pn and pp pairs determines the value of the ratio. A rapid decrease of the pp/pn ratio is seen to start at $k \gtrsim k_F$. For all considered carbon isotopes the SRC pn removal probability is much larger than the pp one for $k_F \lesssim k \lesssim 3k_F$. The dominance of the pn SRC pairs over the pp SRC ones in that momentum range is clearly illustrated in the center panel of Fig. 5. For all carbon isotopes the SRC-driven $p(C, p'pn)$ cross section is at least an order of magnitude larger than the $p(C, p'pp)$ one. We can conclude that for all isotopes, pn pair knockout dominates for $k_F \lesssim k \lesssim 3k_F$, a property that is observed experimentally in electro-induced nucleon pair knockout from ^{12}C [5,44]. For $k \gtrsim 3k_F$ the cross sections are no longer dominated by the tensor correlation function, and the pp over pn SRC-pair probabilities display similar trends as observed for $k \lesssim k_F$. The expected fraction of pn over pp SRC pair removals for $k_F \lesssim k \lesssim 3k_F$ can be defined as

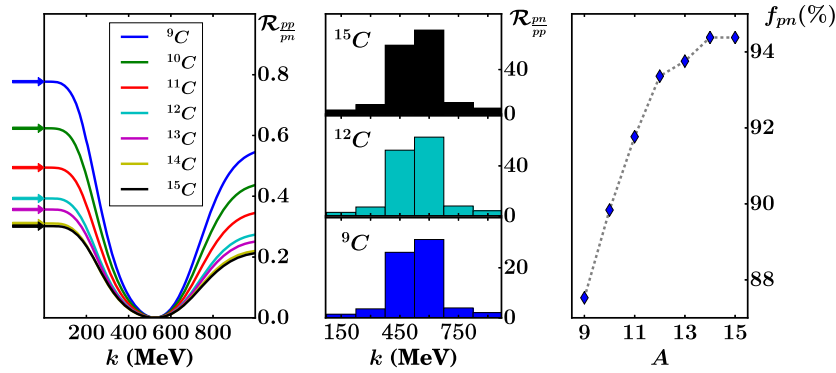


Fig. 5. Ratios of the pn and pp SRC-pair removal probabilities in various carbon isotopes. Left: the pp over pn ratio, this is the reciprocal of Eq. (20), as a function of the initial relative momentum k of the SRC NN pair. The arrows indicate the constant ratio $\frac{1}{2} + \frac{3}{2}S_0$ when no tensor correlations are taken into account. Center: the k dependence of the binned pn over pp ratios of Eq. (20). Right: the fraction of SRC pn pairs defined in Eq. (21) for different carbon isotopes.

$$f_{pn} = \frac{\sum_{\beta\gamma} \int_{k_F}^{3k_F} dk \int d\Omega_k \int d\vec{P} P_{\beta\gamma}^0(\vec{P}, \vec{k})}{\sum_{\beta\gamma} \int_{k_F}^{3k_F} dk \int d\Omega_k \int d\vec{P} [P_{\beta\gamma}^1(\vec{P}, \vec{k}) + P_{\beta\gamma}^0(\vec{P}, \vec{k})]}. \quad (21)$$

In Fig. 5 we display predictions for f_{pn} as a function of A for $Z = 6$. The observed trends can be mainly attributed to the number of ($n = 0, l = 0$) pn and pp pairs for given (N, Z) . For ^{12}C , we find a fraction $\approx 93\%$ that is comparable to the fractions extracted from measurements [44,5]. Our predictions for f_{pn} cover neutron excess values $(N - Z)/Z$ between -0.5 and $+0.5$. Over that range the f_{pn} changes by less than 10%, a value much smaller than anticipated on the basis of variations in the ratio $(N \times Z)/(Z \times Z)$.

4. Conclusions

We have introduced a factorized plane-wave-based model for the calculation of SRC-driven $p(A, p'N_1N_2R^*)$ reaction cross sections, that can serve in particular for the analysis of exclusive proton-induced two-nucleon knockout reactions in inverse kinematics. Our model calculates these cross sections based on a chosen set of single-particle wave functions, correlation functions and free pN -scattering cross section data. We have shown that our model reproduces characteristic features of SRC-driven two-nucleon knockout reactions that are also found in electro-induced two-nucleon knockout reactions. We also describe $^{12}\text{C}(p, p'pn)$ data rather well. Based on the factorization properties of the cross section, we can conclude that the isospin dependence of SRC can be studied by evaluating cross-section ratios. The ratio of the integrated removal probabilities for pn over pp pairs can be connected to a ratio of correlation functions depending on the initial relative momentum of the pair. Our model is an important first step in constructing a reaction model. Required refinements to the proposed model include the description of IFSI and the inclusion of configuration-mixing effects [45] in the description of the ground-state wave function of the target nuclei. The model is applicable to planned experiments aimed at further uncovering the characteristics of nuclear SRC, in particular its asymmetry dependence.

Acknowledgements

The computational resources (Stevin Supercomputer Infrastructure) and services used in this work were provided by the VSC (Flemish Supercomputer Center), funded by Ghent University, FWO and the Flemish Government – department EWI.

References

- [1] J. Arrington, D.W. Higinbotham, G. Rosner, M. Sargsian, Hard probes of short-range nucleon–nucleon correlations, *Prog. Part. Nucl. Phys.* 67 (2012) 898–938, <https://doi.org/10.1016/j.pnpnp.2012.04.002>, arXiv:1104.1196.
- [2] C. Ciofi degli Atti, In-medium short-range dynamics of nucleons: recent theoretical and experimental advances, *Phys. Rep.* 590 (2015) 1–85, <https://doi.org/10.1016/j.physrep.2015.06.002>.
- [3] O. Hen, G.A. Miller, E. Piasetzky, L.B. Weinstein, Nucleon–nucleon correlations, short-lived excitations, and the quarks within, arXiv:1611.09748.
- [4] W.H. Dickhoff, C. Barbieri, Self-consistent Green’s function method for nuclei and nuclear matter, *Prog. Part. Nucl. Phys.* 52 (2004) 377–496, <https://doi.org/10.1016/j.pnpnp.2004.02.038>, arXiv:nucl-th/0402034.
- [5] O. Hen, et al., Momentum sharing in imbalanced Fermi systems, *Science* 346 (2014) 614–617, <https://doi.org/10.1126/science.1256785>, arXiv:1412.0138.
- [6] M.M. Sargsian, New properties of the high-momentum distribution of nucleons in asymmetric nuclei, *Phys. Rev. C* 89 (3) (2014) 034305, <https://doi.org/10.1103/PhysRevC.89.034305>, arXiv:1210.3280.
- [7] R.B. Wiringa, R. Schiavilla, S.C. Pieper, J. Carlson, Nucleon and nucleon-pair momentum distributions in $A \leq 12$ nuclei, *Phys. Rev. C* 89 (2) (2014) 024305, <https://doi.org/10.1103/PhysRevC.89.024305>, arXiv:1309.3794.
- [8] J. Ryckebusch, W. Cosyn, M. Vanhalst, Stylized features of single-nucleon momentum distributions, *J. Phys. G* 42 (5) (2015) 055104, <https://doi.org/10.1088/0954-3899/42/5/055104>, arXiv:1405.3814.
- [9] M. Fortin, C. Providencia, A.R. Raduta, F. Gulminelli, J.L. Zdunik, P. Haensel, M. Bejger, Neutron star radii and crusts: uncertainties and unified equations of state, *Phys. Rev. C* 94 (3) (2016) 035804, <https://doi.org/10.1103/PhysRevC.94.035804>, arXiv:1604.01944.
- [10] M. Oertel, M. Hempel, T. Klähn, S. Typel, Equations of state for supernovae and compact stars, *Rev. Mod. Phys.* 89 (1) (2017) 015007, <https://doi.org/10.1103/RevModPhys.89.015007>, arXiv:1610.03361.
- [11] C.J.G. Onderwater, et al., Dominance of S-01 proton-pair emission in the O-16 (e, e-prime pp) reaction, *Phys. Rev. Lett.* 78 (1997) 4893–4897, <https://doi.org/10.1103/PhysRevLett.78.4893>.
- [12] C. Giusti, F.D. Pacati, K. Allaart, W.J.W. Geurts, W.H. Dickhoff, H. Muther, Selectivity of the O-16(e,e-prime p p) reaction to discrete final states, *Phys. Rev. C* 57 (1998) 1691–1702, <https://doi.org/10.1103/PhysRevC.57.1691>, arXiv:nucl-th/9709021.
- [13] C.J.G. Onderwater, et al., Signatures for short-range correlations in O-16 observed in the reaction O-16 (e, e-prime pp) C-14, *Phys. Rev. Lett.* 81 (1998) 2213–2216, <https://doi.org/10.1103/PhysRevLett.81.2213>.
- [14] G. Rosner, Probing short-range nucleon–nucleon correlations with virtual photons at mami, *Prog. Part. Nucl. Phys.* 44 (2000) 99–112, [https://doi.org/10.1016/S0146-6410\(00\)00063-6](https://doi.org/10.1016/S0146-6410(00)00063-6), <http://www.sciencedirect.com/science/article/pii/S0146641000000636>.
- [15] R. Starink, et al., Evidence for short-range correlations in ^{16}O , *Phys. Lett. B* 474 (2000) 33–40, [https://doi.org/10.1016/S0370-2693\(99\)01510-5](https://doi.org/10.1016/S0370-2693(99)01510-5).
- [16] A. Tang, et al., n-p short range correlations from (p, 2p + n) measurements, *Phys. Rev. Lett.* 90 (2003) 042301, <https://doi.org/10.1103/PhysRevLett.90.042301>, arXiv:nucl-ex/0206003.
- [17] R. Shneor, et al., Investigation of proton–proton short-range correlations via the C-12(e, e-prime pp) reaction, *Phys. Rev. Lett.* 99 (2007) 072501, <https://doi.org/10.1103/PhysRevLett.99.072501>, arXiv:nucl-ex/0703023.
- [18] I. Korover, et al., Probing the repulsive core of the nucleon–nucleon interaction via the $^4\text{He}(e, epN)$ triple-coincidence reaction, *Phys. Rev. Lett.* 113 (2) (2014) 022501, <https://doi.org/10.1103/PhysRevLett.113.022501>, arXiv:1401.6138.

- [19] C. Colle, O. Hen, W. Cosyn, I. Korover, E. Piaszty, J. Ryckebusch, L.B. Weinstein, Extracting the mass dependence and quantum numbers of short-range correlated pairs from $A(e, ep)$ and $A(e, epp)$ scattering, *Phys. Rev. C* 92 (2) (2015) 024604, <https://doi.org/10.1103/PhysRevC.92.024604>, arXiv:1503.06050.
- [20] J. Ryckebusch, Photoinduced two proton knockout and ground state correlations in nuclei, *Phys. Lett. B* 383 (1996) 1–8, [https://doi.org/10.1016/0370-2693\(96\)00725-3](https://doi.org/10.1016/0370-2693(96)00725-3), arXiv:nucl-th/9605043.
- [21] C. Colle, W. Cosyn, J. Ryckebusch, Final-state interactions in two-nucleon knockout reactions, *Phys. Rev. C* 93 (3) (2016) 034608, <https://doi.org/10.1103/PhysRevC.93.034608>, arXiv:1512.07841.
- [22] T. Aumann, Prospects of nuclear structure at the future [GSI] accelerators, in: International Workshop on Nuclear Physics 28th Course Radioactive Beams, Nuclear Dynamics and Astrophysics Ettore Majorana Center for Scientific Culture, *Prog. Part. Nucl. Phys.* 59 (1) (2007) 3–21, <https://doi.org/10.1016/j.ppnp.2006.12.018>, <http://www.sciencedirect.com/science/article/pii/S0146641006000974>.
- [23] T. Kobayashi, et al., (p, 2p) reactions on C-(9–16) at 250-MeV/A, *Nucl. Phys. A* 805 (2008) 431–438, <https://doi.org/10.1016/j.nuclphysa.2008.02.282>.
- [24] V. Panin, et al., Exclusive measurements of quasi-free proton scattering reactions in inverse and complete kinematics, *Phys. Lett. B* 753 (2016) 204–210, <https://doi.org/10.1016/j.physletb.2015.11.082>.
- [25] G. Jacob, T.A.J. Maris, Quasi-free scattering and nuclear structure. 2, *Rev. Mod. Phys.* 45 (1973) 6–21, <https://doi.org/10.1103/RevModPhys.45.6>.
- [26] P. Kitching, W.J. McDonald, T.A.J. Maris, C.A.Z. Vasconcellos, Recent developments in quasifree nucleon–nucleon scattering, *Adv. Nucl. Phys.* 15 (1985) 43–83.
- [27] J. Ryckebusch, V. Van der Sluys, K. Heyde, H. Holvoet, W. Van Nespén, M. Waroquier, M. Vanderhaeghen, Electroinduced two nucleon knockout and correlations in nuclei, *Nucl. Phys. A* 624 (1997) 581–622, [https://doi.org/10.1016/S0375-9474\(97\)00385-0](https://doi.org/10.1016/S0375-9474(97)00385-0), arXiv:nucl-th/9702049.
- [28] K.I. Blomqvist, et al., Investigation of short range nucleon nucleon correlations using the reaction C-12(e,e' p p) in close to 4pi geometry, *Phys. Lett. B* 421 (1998) 71–78, [https://doi.org/10.1016/S0370-2693\(98\)00024-0](https://doi.org/10.1016/S0370-2693(98)00024-0).
- [29] C. Colle, W. Cosyn, J. Ryckebusch, M. Vanhalst, Factorization of exclusive electron-induced two-nucleon knockout, *Phys. Rev. C* 89 (2) (2014) 024603, <https://doi.org/10.1103/PhysRevC.89.024603>, arXiv:1311.1980.
- [30] A.W. Stetz, Analysis of quasi-free scattering data in the impulse approximation, *Phys. Rev. C* 21 (1980) 1979–1988, <https://doi.org/10.1103/PhysRevC.21.1979>.
- [31] R. Guardiola, P.I. Moliner, J. Navarro, R.F. Bishop, A. Puente, N.R. Walet, Translationally invariant treatment of pair correlations in nuclei. 1. Spin and isospin dependent correlations, *Nucl. Phys. A* 609 (1996) 218–236, [https://doi.org/10.1016/0375-9474\(96\)00315-6](https://doi.org/10.1016/0375-9474(96)00315-6), arXiv:nucl-th/9607024.
- [32] O. Benhar, V.R. Pandharipande, S.C. Pieper, Electron-scattering studies of correlations in nuclei, *Rev. Mod. Phys.* 65 (1993) 817–828, <https://doi.org/10.1103/RevModPhys.65.817>.
- [33] S.C. Pieper, R.B. Wiringa, V.R. Pandharipande, Variational calculation of the ground state of O-16, *Phys. Rev. C* 46 (1992) 1741–1756, <https://doi.org/10.1103/PhysRevC.46.1741>.
- [34] C. Ciofi degli Atti, D. Treleani, Linked cluster expansion for the calculation of the semi-inclusive $A(e, e' p) X$ processes using correlated Glauber wave functions, *Phys. Rev. C* 60 (1999) 024602, <https://doi.org/10.1103/PhysRevC.60.024602>.
- [35] M. Vanhalst, J. Ryckebusch, W. Cosyn, Quantifying short-range correlations in nuclei, *Phys. Rev. C* 86 (2012) 044619, <https://doi.org/10.1103/PhysRevC.86.044619>, arXiv:1206.5151.
- [36] C. Gearheart, Ph.D. thesis, Washington University, St. Louis, 1994.
- [37] R.A. Arndt, I.I. Strakovsky, R.L. Workman, Nucleon nucleon elastic scattering to 3 GeV, *Phys. Rev. C* 62 (2000) 034005, <https://doi.org/10.1103/PhysRevC.62.034005>, arXiv:nucl-th/0004039.
- [38] Scattering analysis interactive dial-in program (SAID), <http://gwdac.phys.gwu.edu/>.
- [39] V. Uzhinsky, A. Galoyan, Q. Hu, J. Ritman, H. Xu, Empirical parametrization of the nucleon–nucleon elastic scattering amplitude at high beam momenta for Glauber calculations and Monte Carlo simulations, *Phys. Rev. C* 94 (6) (2016) 064003, <https://doi.org/10.1103/PhysRevC.94.064003>, arXiv:1603.04731.
- [40] T. Van Cuyck, N. Jachowicz, R. González-Jiménez, M. Martini, V. Pandey, J. Ryckebusch, N. Van Dessel, Influence of short-range correlations in neutrino-nucleus scattering, *Phys. Rev. C* 94 (2) (2016) 024611, <https://doi.org/10.1103/PhysRevC.94.024611>, arXiv:1606.00273.
- [41] E. Piaszty, M. Sargsian, L. Frankfurt, M. Strikman, J.W. Watson, Evidence for the strong dominance of proton–neutron correlations in nuclei, *Phys. Rev. Lett.* 97 (2006) 162504, <https://doi.org/10.1103/PhysRevLett.97.162504>, arXiv:nucl-th/0604012.
- [42] A. Malki, et al., Backward emitted high-energy neutrons in hard reactions of p and pi+ on carbon, *Phys. Rev. C* 65 (2002) 015207, <https://doi.org/10.1103/PhysRevC.65.015207>, arXiv:nucl-ex/0005006.
- [43] L.L. Frankfurt, M.I. Strikman, Hard nuclear processes and microscopic nuclear structure, *Phys. Rep.* 160 (1988) 235–427, [https://doi.org/10.1016/0370-1573\(88\)90179-2](https://doi.org/10.1016/0370-1573(88)90179-2).
- [44] R. Subedi, et al., Probing cold dense nuclear matter, *Science* 320 (2008) 1476–1478, <https://doi.org/10.1126/science.1156675>, arXiv:0908.1514.
- [45] M. Makek, P. Achenbach, C.A. Gayoso, C. Barbieri, J.C. Bernauer, R. Boehm, D. Bosnar, A. Denig, M.O. Distler, I. Friscic, C. Giusti, H. Merkel, U. Mueller, L. Nungesser, J. Pochodzalla, S.S. Majos, B.S. Schlimme, M. Schwamb, T. Walcher, A. Collaboration, Differential cross section measurement of the C-12(e, e' pp)Be-10(g.s.) reaction, *Eur. Phys. J. A* 52 (9), <https://doi.org/10.1140/epja/i2016-16298-3>.